

# An Approach for Nonlinear Model Extraction from Time-Series Data

Gregory Hagen and Umesh Vaidya

**Abstract**—We provide a numerical approach to estimating nonlinear stochastic dynamic models from time-series data. After possible dimensional reduction, time-series data can be used to construct an empirical Markov model. Spectral analysis of the Markov model is then carried out to detect the presence of complex limit cycling, almost invariant, and bi-stable behavior in the model. Model parameters are expressed as a linear combination of basis functions over the phase space. A least squares minimization is used to fit the basis function coefficients in order to match the spectral properties of the respective Markov operators. The approach is demonstrated on the estimation of a nonlinear stochastic model describing combustion oscillation data.

## I. INTRODUCTION

This paper is concerned with reduced order modeling of the dynamical systems exhibiting complex behavior and whose description is available in the form of time series data. In many problems of applied interest the system information is available in the form of time series data, which is typically of large dimension. Examples includes problems in turbulent fluid flows, climate and weather prediction, systems biology, social and behavioral modeling, cognitive measurement, bio-sensing and applications involving large numbers of sensors and actuators. Reduced order models for all the data driven application will help in more accurate analysis, prediction, and more precise control. Models from measurement can also guide the measurement process, and determine when, where and how it is best to gather additional data, has itself the potential of enabling more effective measurement methodologies.

In the present paper, we provide an approach for estimating nonlinear dynamic models, possibly driven by noise. The estimation approach is based on comparing the spectral properties of the empirically constructed Markov operator with the model-based Markov operator. A nonlinear model is fit such that its associated Markov operator has similar spectral properties as the empirical Terms in the stochastic differential equation model are estimated by a linear combination of basis functions. The coefficients appear in the numerical approximation of the Markov model, and are fit using least squares minimization. Model validation is motivated spectral methods developed in [5] [4] for the comparison of dynamical systems.

This paper is organized as follows. In section II, we describe the spectral methods for the analysis and comparison of dynamical systems. In section III we outline an approach

to numerically approximate the stochastic dynamical system (1) based on the empirically obtained Markov matrix  $P$ . In section IV the techniques are illustrated on the estimation of a nonlinear stochastic differential equation model of unsteady combustion oscillations.

## II. SPECTRAL METHOD FOR ANALYSIS AND COMPARISON

In this section, we describe spectral methods for the analysis and comparison of the dynamical systems. The material for this section is taken from [2][5][4]. Also, see [3] for an introduction to these concepts.

Consider the stochastic dynamical system

$$\frac{\partial x}{\partial t} = b(x) + \sigma(x)\xi, \quad x \in X \subset \mathbb{R}^d, \quad (1)$$

or its discrete time equivalent,

$$x_{k+1} = T(x_k, \xi_k) \quad (2)$$

where each  $x_k \in X \subset \mathbb{R}^d$  is the state vector and  $\xi_k \in U$  is sequence of i.i.d. random noise. Associated with  $T$  is a stochastic transition function  $p(x, A)$ , which gives the transition probability to jump from point  $x \in X$  to set  $A \in \mathcal{B}(X)$ , where  $\mathcal{B}(X)$  is the Borel sigma algebra of  $X$ . For deterministic dynamics i.e., when  $\xi_n = 0$ , we have  $p(x, A) = \delta_{T(x)}(A)$ , where  $\delta$  is the Dirac delta measure. Stochastic transition function can be used to define two linear transfer operators called as Perron-Frobenius and Koopman operator defined as follows

*Definition 1 (Perron-Frobenius operator):* The Perron-Frobenius (P-F) operator  $\mathbb{P} : \mathcal{M}(X) \rightarrow \mathcal{M}(X)$  corresponding to  $p(x, A)$  is defined by

$$\mathbb{P}[\mu](A) = \int_X p(x, A) d\mu(x). \quad (3)$$

where  $\mathcal{M}(X)$  is the vector space of all measures on  $X$ . For deterministic dynamics, the P-F operator is given by

$$\mathbb{P}[\mu](A) = \int_X \delta_{T(x)}(A) d\mu(x) = \int_X \chi_A(Tx) d\mu(x) = \mu(T^{-1}(A)) \quad (4)$$

where  $\chi_A(\cdot)$  is the indicator function with support on  $A$ , and  $T^{-1}(A)$  is the pre-image set.

*Definition 2 (Koopman Operator):*  $\mathbb{U} : \mathcal{C}^0(X) \rightarrow \mathcal{C}^0(X)$  is defined by

$$(\mathbb{U}f)(x) = \int_X p(x, dy) f(y) \quad (5)$$

where  $\mathcal{C}^0(X)$  is the space of all continuous function.

For deterministic dynamics Koopman operator is given by

$$(\mathbb{U}f)(x) = f(T(x)) \quad (6)$$

G. Hagen is with United Technologies Research Center, East Hartford, CT 06108. hagen@utrc.utc.com

U. Vaidya is with the Department of Electrical & Computer Engineering, Iowa State University, Ames, IA 50011 ugvaiddya@iastate.edu

So the P-F operator is used to propagate the sets or the measure supported on the sets in the forward direction and the Koopman operator is used to propagate functions in backward direction. Perron-Frobenius and Koopman operators are dual to each other and the duality is expressed using the following inner product [3]

$$\langle \mathbb{U}f, \mu \rangle_X = \langle f, \mathbb{P}\mu \rangle_X$$

Global transport properties of a nonlinear system can be very effectively studied using P-F and Koopman operators. In particular, complex behavior such as chaotic attractor, limit cycles, periodic orbits, almost invariant and bistable behavior can be easily characterized using eigenvalues and eigenvectors of these operators [2][1][6]. This dynamical analysis of a nonlinear systems can be carried out by considering the finite dimensional approximation of the operators. Here we consider the finite dimensional approximation of the P-F operator. To do this we consider the finite partition of the state space  $X$  i.e.,

$$\mathcal{X} = \{D_1, \dots, D_m\} \quad (7)$$

such that  $D_i \cap D_j = \emptyset$  for  $i \neq j$  and  $\cup_{i=1}^m D_i = X$ . This finite partition can be used to identify the infinite dimensional measure space to finite dimensional vector space  $\mathbb{R}^m$ , each box  $D_i$  can be associated with a number  $\mu_i$  and the measure  $\mu \in \mathcal{M}(X)$  can be approximated as

$$d\mu(x) = \sum_{i=1}^m \mu_i \chi_i(x) \frac{d\mu_L(x)}{\mu_L(D_i)}$$

where  $\chi_i(x)$  is the indicator function on set  $D_i$  and  $\mu_L$  is the Lebesgue measure. P-F operator on the finite dimensional vector space  $\mathbb{R}^m$  can be represented by a matrix  $P: \mathbb{R}^m \rightarrow \mathbb{R}^m$  as follows:

$$P_{ij} = \frac{\mu_L(T^{-1}(D_j) \cap D_i)}{\mu_L(D_i)}, \quad i, j = 1, \dots, m \quad (8)$$

The resulting matrix is non-negative and because  $T: D_i \rightarrow X$ ,  $\sum_{j=1}^m P_{ij} = 1$  i.e.,  $P$  is a Markov or a row-stochastic matrix. In the present case, the entries of the matrix  $P$  are computed from the time-series data. Computationally, several short term trajectories are used to compute the individual entries  $P_{ij}$ . The mapping  $T$  is used to transport  $M$  "initial conditions" chosen to be uniformly distributed within a set  $D_i$ . The entry  $P_{ij}$  is then approximated by the fraction of initial conditions that are in the box  $D_j$  after one iterate of the mapping.

Important complex dynamical features of the dynamical system  $T$  can be captured using its Markov matrix  $P$ . For example long term or asymptotic behavior of the dynamical system  $T$  is captured by the invariant measure or more appropriately physically relevant measure. Finite dimensional approximation of the invariant measure or the outer approximation to the support of the invariant measure can be obtain from the left eigenvector of Markov matrix  $P$  with eigenvalue one. i.e.,

$$\mu P = 1 \cdot \mu$$

Similarly the presence of periodic or limit cycling behavior in  $T$  can be captured by the complex unitary spectrum and the corresponding eigenvectors of  $P$ . Moreover if the Markov matrix  $P$  has real eigenvalue close to one then it is the indicator for the presence of almost invariant or bistable behavior in the dynamical system  $T$ . For more detail on this topic refer to [1][2].

Now we provide a brief overview of some of the key results from [5] and [4] on spectral methods based on Koopman and P-F operator for model comparison. The key idea proposed in these paper is that the model comparison involving comparison of time averages or the invariant measures fail to capture the essential spectral characteristics of the possible behavior. This essential spectral characteristics can be captured in two different ways: either by computing the harmonic averages, which is the subject of study in [5], or by computing the eigenmeasure corresponding to the complex unitary spectrum of the P-F operator as done in [4]. Both these approaches lead to the same result. An pseudometric between dynamical systems can be constructed by appropriately chosen distance function between the harmonic averages or the eigenmeasure corresponding to complex unitary eigenvalues. In [5], harmonic averages are constructed as follows. For the partition  $\mathcal{X}$  of the phase space  $X$ , let  $\chi_j(x)$  be the indicator function for the set  $D_j$ . Harmonic average for a given normalized frequency  $\omega$  and corresponding  $\lambda = e^{i2\pi\omega}$  is constructed using Koopman operator as follows

$$\chi_{j,\lambda(\omega)}^* = \frac{1}{N} \sum_{k=0}^{N-1} \lambda^k (\mathbb{U}^k \chi_j)(x_0)$$

If the system has a periodic orbit of period  $\omega^*$ , then harmonic averages for all  $\lambda$ , except for the one corresponding to  $\omega^*$  will be zero. This frequency  $\omega$  can be obtained by performing the DFT of the signal first. In [4], it is shown that

$$\chi_{j,\lambda(\omega)}^* = \mu_j^{\lambda(\omega)}$$

where  $\mu_j^\lambda$  is the  $j$  component of the eigenvector of  $P$  with complex unitary eigenvalue  $\lambda = e^{i2\pi\omega}$  i.e.,

$$\mu^\lambda P = \lambda \mu \quad \mu^\lambda = (\mu_1^\lambda, \dots, \mu_m^\lambda)$$

Hence instead of using the harmonic averages one can also use the eigenvector corresponding to complex unitary eigenvalues in the construction of pseudometric on the space of dynamical systems.

### III. NUMERICAL APPROACH FOR MODEL IDENTIFICATION

We outline an approach to numerically approximate the stochastic dynamical system (1) based on the empirically obtained Markov matrix  $P$ .

Set

$$a_{ij}(x) = \sum_{k=1}^d \sigma_{ik}(x) \sigma_{jk}(x) \quad (9)$$

Under certain regularity conditions [3], the evolution of the density,  $\rho$  under (1) satisfies the Fokker-Planck equation,

$$\begin{aligned} \frac{\partial \rho}{\partial t} &= \frac{1}{2} \sum_{i,j=1}^d \frac{\partial^2}{\partial x_i \partial x_j} (a_{ij} \rho) - \sum_{i=1}^d \frac{\partial}{\partial x_i} (b_i \rho) \\ &:= \mathcal{F} \rho, \quad t > 0, x \in \mathbb{R}^d. \end{aligned} \quad (10)$$

Let us consider the finite-dimensional (discrete-space) approximation of  $\mathcal{F}$  by discretizing the underlying phase space  $X$  with the partition  $\mathcal{X}$  following (7). Therefore, the distribution  $\rho$  is approximated by a finite-dimensional vector  $u(x) \in \mathbb{R}^m$  and let

$$U = \text{diag}\{u\} \in \mathbb{R}^{m \times m}, \quad (11)$$

where  $\text{diag}\{u\}$  is a diagonal matrix whose entries are the elements of the vector  $u$ . Similarly, the operators are approximated by their finite-dimensional matrices:

$$F \approx \mathcal{F}, \quad F \in \mathbb{R}^{m \times m}.$$

Continuing this way, write the discretized approximations of  $a_{ij}(x)$  and  $b_i(x)$ , respectively,

$$a_{ij}(x) \approx A_{ij}(x) \in \mathbb{R}^m, \quad b_i(x) \approx B_i(x) \in \mathbb{R}^m. \quad (12)$$

Similarly we write the discretized differential operators

$$\frac{1}{2} \frac{\partial^2}{\partial x_i \partial x_j} \approx D_{ij}^2 \in \mathbb{R}^{m \times m}, \quad \frac{\partial}{\partial x_i} \approx D_i \in \mathbb{R}^{m \times m}. \quad (13)$$

Next, define the matrices:

$$D^2(U) := [D_{11}^2 U, \dots, D_{ij}^2 U, \dots, D_{dd}^2 U] \in \mathbb{R}^{m \times md^2} \quad (14)$$

$$D^1(U) := [D_1 U, \dots, D_i U, \dots, D_d U] \in \mathbb{R}^{m \times md} \quad (15)$$

$$D(U) := [D^2(U), D^1(U)] \in \mathbb{R}^{m \times (md^2 + md)} \quad (16)$$

and

$$\begin{aligned} A &:= \begin{bmatrix} A_{11} \\ \vdots \\ A_{ij} \\ \vdots \\ A_{dd} \end{bmatrix} \in \mathbb{R}^{md^2}, \quad B := \begin{bmatrix} B_1 \\ \vdots \\ B_j \\ \vdots \\ B_d \end{bmatrix} \in \mathbb{R}^{md}, \\ C &:= \begin{bmatrix} A \\ B \end{bmatrix} \in \mathbb{R}^{(md^2 + md)}. \end{aligned} \quad (17)$$

The infinite-dimensional Fokker-Planck operator is approximated in finite dimensions by

$$\mathcal{F} \rho \approx F u = D(U) C. \quad (18)$$

We next write (10) in discrete time, with

$$\frac{\partial u}{\partial t} \approx \frac{u_{t+1} - u_t}{\delta t},$$

where  $\delta t$  is the time step which the time-series data was obtained. Substituting this into the left side of (10) results in the Markov matrix appearing equation (8),

$$\begin{aligned} u_{t+1} &= u_t + \delta t F u_t \\ &= [u_t + \delta t D(U) C] \\ &:= P u_t. \end{aligned} \quad (19)$$

We empirically obtain  $P$  directly from data by discretizing the underlying phase space ( $\mathbb{R}^d$ ) to obtain this discrete-space approximation. The spectrum of  $P$  is given by  $P \mathcal{V} = \mathcal{V} \Lambda$ , where

$$\mathcal{V} = [v_0, v_1, v_2, \dots, v_m], \quad \Lambda = \text{diag}(\lambda_0, \lambda_1, \dots, \lambda_m). \quad (20)$$

Under suitable conditions there exists a steady distribution  $v_0$  where  $\lambda_0 = 1$ .

Consider a single eigenvector  $v \in \mathbb{R}^m$  with eigenvalue  $\lambda$ . We have

$$P v = [v + \delta t D(V) C] = \lambda v, \quad (21)$$

and after rearranging,

$$D(V) C = \frac{\lambda - 1}{\delta t} v := w. \quad (22)$$

This can be solved for  $C$  which will give the functional forms of  $b(x)$  and  $\sigma(x)$  appearing in (1). Of course, for a single eigenvector, there are multiple solutions. We solve (22) for multiple eigenpairs; the first  $k$  for example. We have

$$\begin{bmatrix} D(V_0) \\ \vdots \\ D(V_{k-1}) \end{bmatrix} C = \begin{bmatrix} w_0 \\ \vdots \\ w_{k-1} \end{bmatrix}. \quad (23)$$

Again, for  $k$  small, there are multiple solutions. We next restrict  $C$  to be a linear combination of  $k$  basis functions. Let  $\{\phi_j\}$  be a set of basis functions where  $\phi_j: \mathbb{R}^d \rightarrow \mathbb{R}$ ,  $j = 0, 1, 2, \dots, n-1$ , such as Hermite polynomials. Define the matrix consisting of these basis functions as column vectors:

$$\Phi := [\phi_0, \phi_1, \dots, \phi_{n-1}] \in \mathbb{R}^{m \times n}. \quad (24)$$

We rewrite (17) in terms of these basis functions. For each  $i, j$  take

$$A_{ij} = \Phi \alpha_{ij}, \quad \alpha_{ij} \in \mathbb{R}^n, \quad (25)$$

$$B_i = \Phi \beta_i, \quad \beta_i \in \mathbb{R}^n, \quad (26)$$

and

$$\begin{aligned} \alpha &:= \begin{bmatrix} \alpha_{11} \\ \vdots \\ \alpha_{ij} \\ \vdots \\ \alpha_{dd} \end{bmatrix} \in \mathbb{R}^{nd^2}, \quad \beta := \begin{bmatrix} \beta_1 \\ \vdots \\ \beta_j \\ \vdots \\ \beta_d \end{bmatrix} \in \mathbb{R}^{nd}, \\ c &:= \begin{bmatrix} \alpha \\ \beta \end{bmatrix} \in \mathbb{R}^{(nd^2 + nd)}. \end{aligned} \quad (27)$$

As in (14-16), define the differential operators restricted to these basis functions:

$$D_{\Phi}^2(U) := [D_{11}^2 U \Phi, \dots, D_{ij}^2 U \Phi, \dots, D_{dd}^2 U \Phi] \in \mathbb{R}^{m \times nd^2} \quad (28)$$

$$D_{\Phi}^1(U) := [D_1 U \Phi, \dots, D_i U \Phi, \dots, D_d U \Phi] \in \mathbb{R}^{m \times nd} \quad (29)$$

$$D_{\Phi}(U) := [D_{\Phi}^2(U), D_{\Phi}^1(U)] \in \mathbb{R}^{m \times (nd^2 + nd)}. \quad (30)$$

Rewrite equation (23) as

$$D_{\Phi,k}c := \begin{bmatrix} D_{\Phi}(V_0) \\ \vdots \\ D_{\Phi}(V_{k-1}) \end{bmatrix} c = \begin{bmatrix} w_0 \\ \vdots \\ w_{k-1} \end{bmatrix} := W_k, \quad (31)$$

where  $D_{\Phi,k} \in \mathbb{R}^{km \times (nd^2 + nd)}$ ,  $c \in \mathbb{R}^{(nd^2 + nd)}$ ,  $W_k \in \mathbb{R}^{km}$ .

We solve for  $c$  through least squares:

$$\min_c [D_{\Phi,k}c - W_k]^* [D_{\Phi,k}c - W_k], \quad (32)$$

which results in

$$c = [D_{\Phi,k}^* D_{\Phi,k}]^{-1} D_{\Phi,k}^* W_k. \quad (33)$$

We would like to compare the eigenfunctions of the approximated model with the eigenfunctions appearing in equation (20). We compute the approximate Markov matrix:

$$\hat{D}(c) := \sum_{i,j=1}^d D_{ij}^2 \text{diag}\{\Phi\alpha_{ij}\} + \sum_{i=1}^d D_{ij} \text{diag}\{\Phi\beta_i\}. \quad (34)$$

The approximate Markov matrix is then

$$\hat{P} = I + \delta t \hat{D}(c). \quad (35)$$

We then compare the spectrum of  $\hat{D}(c)$  with the spectrum in (20).

#### IV. APPLICATION EXAMPLE

In this section, we construct a reduced order model describing nonlinear oscillations of flame dynamics. High-speed video data was obtained from the UTRC combustion rig described in [7], and proper orthogonal decomposition (POD) was used for dimension-reduction. We briefly describe how the Markov matrix was empirically constructed.

##### A. Data Reduction using POD Modes

From the image data, the mean field was removed from each of the images and the POD modes were computed. It was found that the first two POD modes account for more than 80% of the energy found in the data set. Hence, we consider a two dimensional state space  $x \in \mathbb{R}^2$ . The two-dimensional time series is constructed via

$$x_k = \begin{bmatrix} x_{1,k} \\ x_{2,k} \end{bmatrix} = \begin{bmatrix} \langle \phi_1, \tilde{y}_k \rangle \\ \langle \phi_2, \tilde{y}_k \rangle \end{bmatrix} \quad (36)$$

where  $\tilde{y}_k$  denotes the  $k$ -th image with the mean field subtracted.

The time series of POD coefficients, given by  $\{x_k\}$ , were obtained from projecting the original data onto the POD modes. The resulting phase space (plotting  $x_{1,k}$  vs.  $x_{2,k}$ , for  $k = 1, \dots, N$ ) is shown in figure (1). The phase portrait shows a noisy limit cycle where the density of points is clearly non-uniform. The rotational speed of the limit-cycle varies depending on the state. This indicates that a nonlinear model is necessary to match this time series.

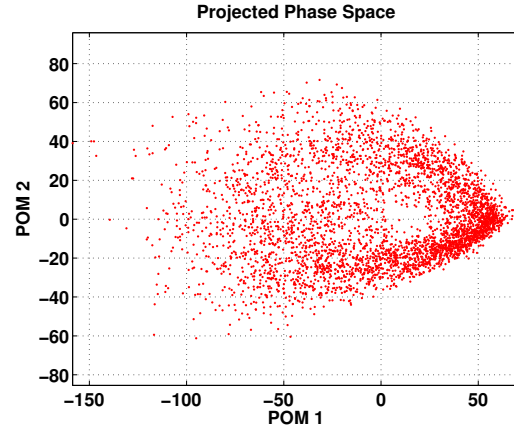


Fig. 1. The phase space of the coefficients resulting from projection of the data onto the first two POD modes

##### B. Empirical Markov Model

A Markov model was computed from this time series data through equation (8). The result is a non-reversible Markov model with many eigenvalues, as shown in Figure 2. Note that the eigenvalues can be collapsed toward the origin by taking powers of  $P$ . The eigenvector corresponding to the unit eigenvalue, shown in Figure 3 confirms the steady distribution of the trajectories.

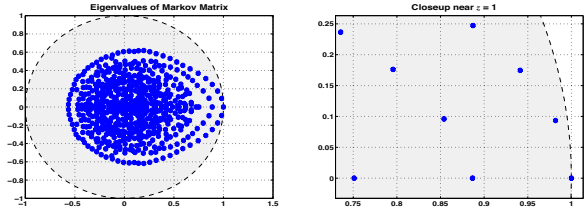


Fig. 2. The eigenvalues of the Markov model.

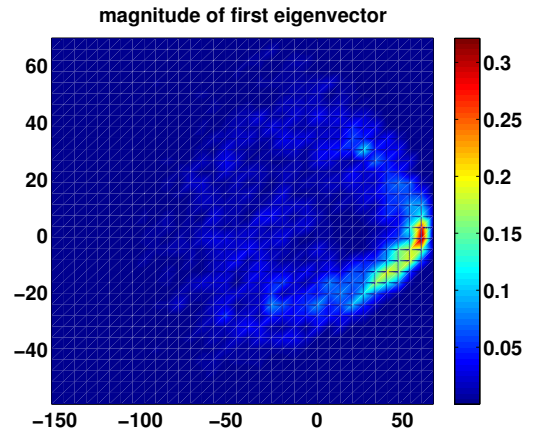


Fig. 3. The first eigenvector shows the invariant distribution

The phase of the eigenvector associated with the 2nd eigenvalue is shown in Figure 4. It reveals the oscillatory nature

of the dynamics.

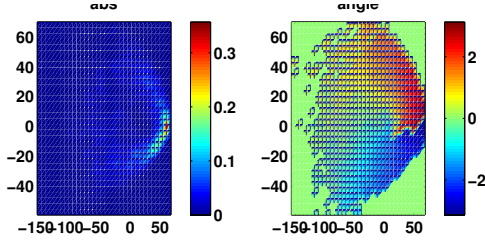


Fig. 4. Magnitude(left) and phase(right) of the second eigenvector

### C. Nonlinear Model Extraction

In this section we develop a second order stochastic differential equation model of the form

$$\begin{aligned} \dot{x}_1 &= b_1(x_1, x_2) + \sigma_{11}\xi_1 \\ \dot{x}_2 &= b_2(x_1, x_2) + \sigma_{22}\xi_2 \end{aligned} \quad (37)$$

to capture the essential dynamical behavior of the reduced set of data from the previous section.

Before going into the details of the model we would like to summarize some of the key dynamical features of the reduced set of data as captured by phase portrait in Figure 1.

- Dynamics consist of stable limit cycle where the motion along the limit cycle is in clockwise direction.
- The limit cycle is parameterized by angle  $\theta$ . Speed along the limit cycle is nonuniform, speed of the limit cycle is less for  $\theta \in [0, -\frac{\pi}{2}]$  compared to other value of  $\theta$ .

We would like the model to capture this essential dynamical behavior along with the amplitude of the limit cycle and the average speed or the frequency of the limit cycle. We choose a reduced set of eigenvalues closest to the unit circle to approximate the Markov model. Due to the cyclic nature of the data, we use basis functions  $\Phi$  in radial coordinates, expressed as separable functions in  $r$  and  $\theta$

$$\begin{aligned} \phi_{k,0}(x_1, x_2) &= r^k \\ \phi_{k,2j}(x_1, x_2) &= r^k \cos(j\theta) \\ \phi_{k,2j+1}(x_1, x_2) &= r^k \sin(j\theta), \\ k &= 0, 1, 2, \dots, j = 0, 1, 2, \dots \end{aligned}$$

where

$$\begin{aligned} x_1 &= r \cos \theta \\ x_2 &= r \sin \theta \end{aligned}$$

The least squares fit (33) resulted in basis function coefficients producing the terms appearing on the right hand side of (37). The functions  $b_1(x_1, x_2)$  and  $b_2(x_1, x_2)$  appear in Figures 5 and 6, respectively. The resulting functions  $\sigma_{11}(x_1, x_2)$  and  $\sigma_{22}(x_1, x_2)$  are qualitatively similar. The resulting approximate eigenfunctions of the estimated Markov matrix are shown in Figure 7 and 8. Figure 7 shows

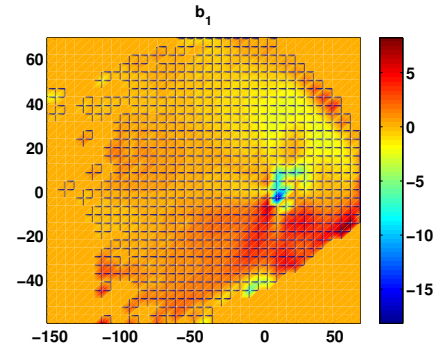


Fig. 5. The estimated  $b_1(x_1, x_2)$  appearing in (37).

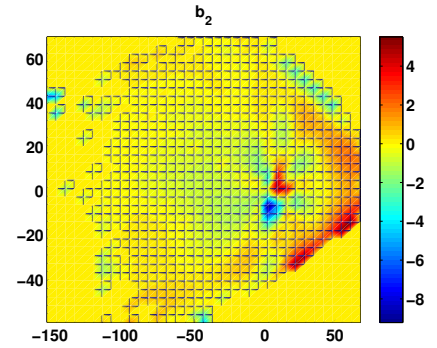


Fig. 6. The estimated  $b_2(x_1, x_2)$  appearing in (37).

the approximate invariant distribution which closely resembles that shown in Figure 3. Similarly, the second complex-valued approximate eigenfunction is shown in Figure 8 which closely resembles the second eigenfunction shown in Figure 4. The match in the eigenfunction indicates a good match between the model and the data in terms of long term dynamics.

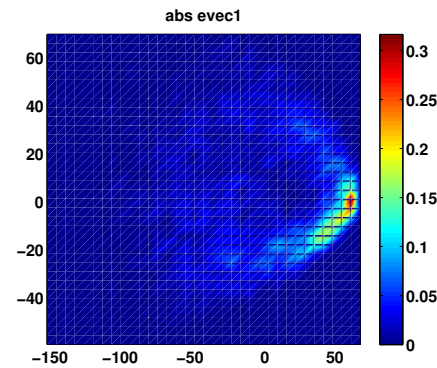


Fig. 7. The approximate first eigenvector of the estimated Markov matrix

## V. CONCLUSION AND DISCUSSION

This paper present results on the construction of reduced order model from a time series data obtained from a experiments. After possible dimensionality reduction, a low-dimensional phase space is identified. We construct a non-

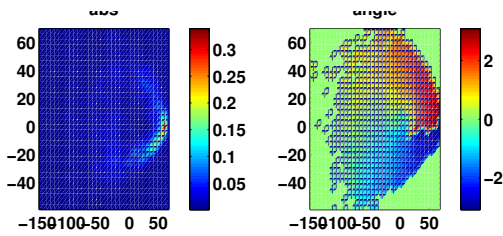


Fig. 8. The approximate magnitude(left) and phase(right) of the second eigenvector of the estimated Markov matrix

linear stochastic differential equation model on the lower dimensional phase space. Terms on the right hand side of the differential equation model are approximated by a linear combination of suitable basis functions. The coefficients are estimated through numerical approximation of the Markov operator, and a least squares fit of basis function coefficients. Model validation is conducted using spectral methods developed in [5] [4] for the comparison of dynamical systems. Parameters of the model are identified such that the time series data generated by the model and from the experiment are close under the pseudometric provided by the spectral method. The proposed approach for reduced order modeling is applied to estimating a nonlinear model describing unsteady combustion dynamics. Future research efforts may focus on determining optimal basis function for the approximation, including forcing terms to the model, and applying the techniques to identify hidden Markov models.

#### ACKNOWLEDGEMENTS

The authors would like to thank Karen Teerlinck at UTRC for providing dynamic data and Igor Mezić at UC Santa Barbara for helpful discussions. The first author was supported in part by AFOSR contract FA9550-07-C-0045 and the second author was supported by Iowa State University grant, which is gratefully acknowledged.

#### REFERENCES

- [1] M. Dellnitz and O. Junge. On the approximation of complicated dynamical behavior. *SIAM Journal on Numerical Analysis*, 36:491–515, 1999.
- [2] M. Dellnitz and O. Junge. *Set oriented numerical methods for dynamical systems*, pages 221–264. World Scientific, 2000.
- [3] A. Lasota and M. C. Mackey. *Chaos, Fractals, and Noise: Stochastic Aspects of Dynamics*. Springer-Verlag, New York, 1994.
- [4] P. G. Mehta and U. Vaidya. On stochastic analysis approaches for comparing dynamical systems. In *Proceeding of IEEE Conference on Decision and Control*, pages 8082–8087, Spain, 2005.
- [5] I. Mezić and A. Banaszuk. Comparison of systems with complex behavior. *Physica D*, 197:101–133, 2004.
- [6] I. Mezić and S. Wiggins. A method for visualization of invariant sets of dynamical systems based on ergodic partition. *Chaos*, 9(1):213–218, 1999.
- [7] K. A. Teerlinck, G. Hagen, A. Banaszuk, J. A. Lovett, J. M. Cohen, A. Ateshkadi, and B. V. Kiel. Demonstration of thermoacoustic instability control in a three-flameholder combustor. *53rd JANNAF (Joint Army-Navy-NASA-Air Force) Propulsion Meeting, Monterey, CA, Dec 5-8, 2005*.